Analysis of Neutral Transport in GAMMA 10 SMBI Experiments*)

Katsuhiro HOSOI, Yousuke NAKASHIMA, Shinji KOBAYSHI[1)], Nobuhiro NISHINO[2)], Tohru MIZUUCHI[1)], Takashi ISHII, Kazuya ICHIMURA, Hisato TAKEDA, Hideaki UEDA, Satoru KIGURE, Shigehito TAKAHASHI, Satoru HOTAKA and Tsuyoshi IMAI

Plasma Research Center, University of Tsukuba, Tsukuba 305-8577, Japan
[1)]*Institute of Advance Energy, Kyoto University, Uji 611-0011, Japan*
[2)]*Grauate School of Engineering, Hiroshima University, Higashihiroshima 739-8527, Japan*

(Received 9 December 2011 / Accepted 6 July 2012)

Results of supersonic molecular beam injection (SMBI) into GAMMA 10 are described. By analyzing the two-dimensional image of the emission captured by a high-speed camera, we investigated neutral transport during SMBI. The experimental results show that the degree of diffusion of the injected neutral particles decreases with increasing plenum pressure. By applying a three-dimensional Monte-Carlo simulation to GAMMA 10, we analyze the neutral-particle transport. The simulation given under the initial conditions of the conventional gas puffing could not reproduce the experimental results. Compared with experimental results, the results of simulation were too diffusive. The experimental SMBI results were roughly reproduced under more squeezed divergence angle of injected particles than that of a cosine distribution. These results reveal a difference between divergence angles for particles launched via SMBI and via conventional gas puffing.

Keywords: GAMMA 10, supersonic molecular beam injection, DEGAS, Hα, high-speed camera

DOI: 10.1585/pfr.7.2402126

1. Introduction

The proper control of gas fueling is very important for obtaining high-density plasmas that perform well. Control of fueling enables optimization of the core-plasma density, which leads to fewer neutral particles dispersed in the peripheral area. Although the technique of ice pellet injection is known to lead to favorable fueling, it is successful only in rather large devices. In addition, in small devices it is not easy to make a pellet small enough to control the core-plasma density. Supersonic molecular beam injection (SMBI), which was developed by L.Yao *et al.* [1], constitutes a new method of gas fueling. SMBI provides high-speed and high-directive gas injection by using a plenum pressure higher than what is used in conventional gas puffing, so that neutral particles can be injected deeper into the core plasma. SMBI has been successfully applied to some devices [2, 3] and is considered especially effective for small and relatively low-density devices such as GAMMA 10.

GAMMA 10 is an open magnetic plasma-confining device [4]. SMBI occurs at the bottom of the central-cell at mid-plane. The central-cell has a simple solenoidal magnetic configuration that uses ten pancake coils. In addition, GAMMA 10 provides many observation ports for observing the central-cell. Thus, during SMBI, the plasma can be observed in the central-cell. The first experimental results of SMBI showed that, compared with conventional gas puffing, this technique leads to higher-density plasmas at the core region. The purpose of the present study is to investigate, both experimental and by simulation, the characteristic of neutral particles during SMBI. To investigate the neutral particles, the emission from the plasma was captured by a high-speed camera. In addition, we investigated how SMBI depends on the plenum pressure. The strategy of the simulation was to compare the results obtained under initial conditions, corresponding to conventional gas puffing, with experimental results. This approach allowed us to derive the optimal initial condition for SMBI.

2. Experimental Set Up

Figure 1 shows a schematic of GAMMA 10, which consists of a central-cell, anchor-cells, plug/barrier-cells and end-cells. The origin $z = 0$ cm is located mid-plane in the central-cell and west and east correspond to plus and minus along the z-axis, respectively. The central-cell is the main region in which the plasma is confined. Mirror-throat regions between the central-cell and anchor-cell contain the first mirror with strong magnetic fields for confining the plasma in the central-cell. The initial plasma is produced by plasma guns located at both ends. Then plasma is produced and heated by ion cyclotron-rang-frequency (ICRF) waves. Two conventional gas-puff systems are installed for sustaining the plasma at both mirror-throat regions.

Figure 2 shows a cross-section of the GAMMA 10 central-cell, a layout of the SMBI system, and the objective

author's e-mail: hosoi_katsuhiro@prc.tsukuba.ac.jp
*) This article is based on the presentation at the 21st International Toki Conference (ITC21).

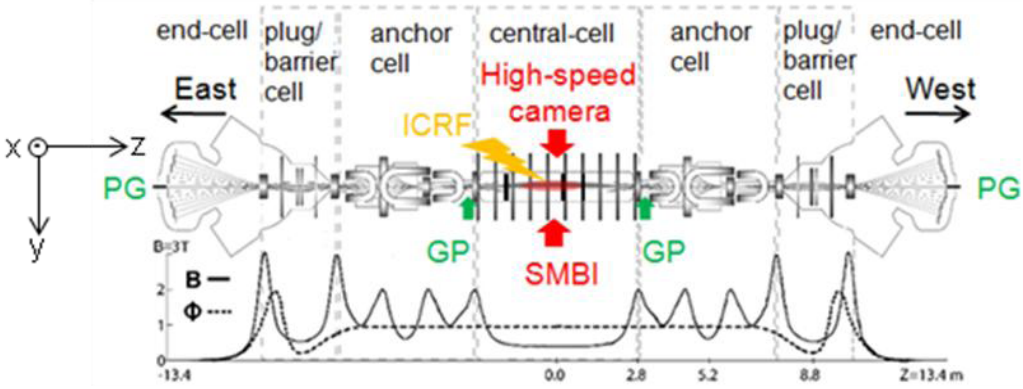

Fig. 1 Schematic of GAMMA 10 and axial profile of magnetic field strength B and potential ϕ. The positions of the various components of the experimental apparatus are shown.

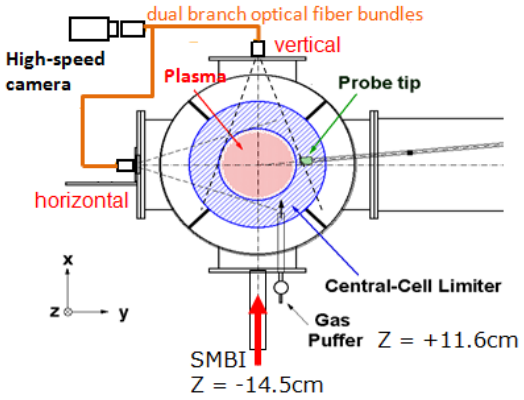

Fig. 2 Schematic of central-cell cross-section and locations of SMBI system and high-speed camera.

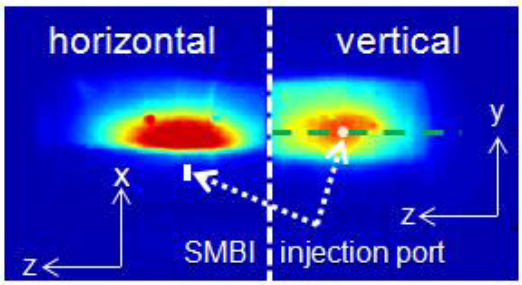

Fig. 3 Two-dimensional images of plasma during SMBI.

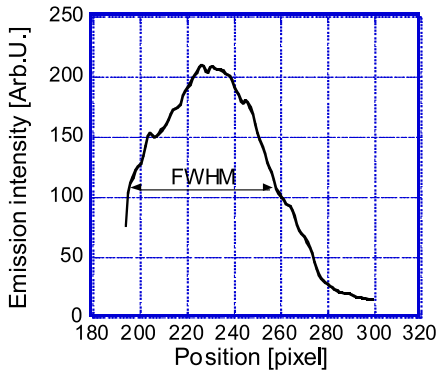

Fig. 4 Distribution of vertical emission intensity obtained by high-speed camera.

optical system for the high-speed camera. A high-speed camera is installed at central-cell to observe the plasma near the central limiter. The high-speed camera observes the two-dimensional (2-D; i.e., x-z, or y-z) response of the plasma to SMBI and is sufficiently capable of measuring visible-light emission. By using dual blanch optical fiber bundles, the camera system has a line of sight in the horizontal direction and one in the vertical direction of the plasma cross-section. The expansion of the molecular beam injected by SMBI in the axial (z) direction and its penetration depth into the plasma can be estimated from the 2-D image in two directions. The SMBI system consists of a fast solenoid valve with a magnetic shield. The plenum pressure is usually 1 MPa and the pulse width is 0.5 to −1.0 ms.

3. Experimental Results

In this experiment, a SMBI pulse was injected into typical plasmas heated only by ICRF. Figure 3 shows a typical 2-D image captured by the high-speed camera of visible emission during SMBI from a GAMMA 10 plasma. These 2-D images were captured at the peak emission intensity. The left side of Fig. 3 shows the intensity emitted in the horizontal direction; the right side shows that emitted in the vertical direction. To investigate the directivity of the molecular beam injected by SMBI, we investigated the axial profile of the neutral transport by using the 2-D vertical-direction image. We also investigated the distribution of emission intensity at the broken line on the right side of Fig. 3 (the broken line was drawn over the SMBI injection port). Figure 4 shows the distribution of emission intensity at the broken line as obtained from the 2-D image in Fig. 3. We used the full width at half maximum (FWHM) of the distribution emission intensity in Fig. 4 as

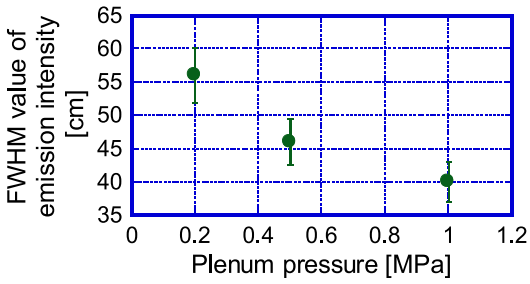

Fig. 5 Emission FWHM (obtained by 2-D image) versus plenum pressure.

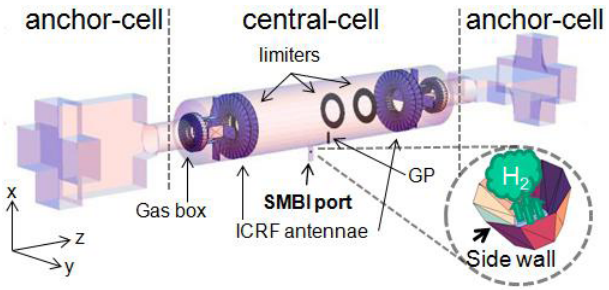

Fig. 6 Fully three-dimensional DEGAS mesh model including SMBI port and region near SMBI valve.

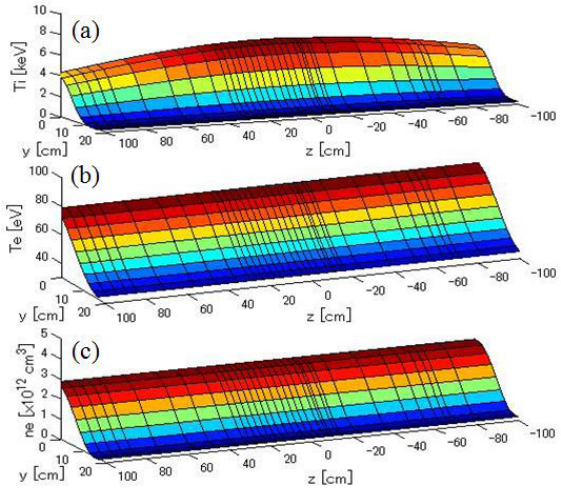

Fig. 7 Input plasma parameters applied to DEGAS simulation: (a) ion temperature, (b) electron temperature, (c) electron density.

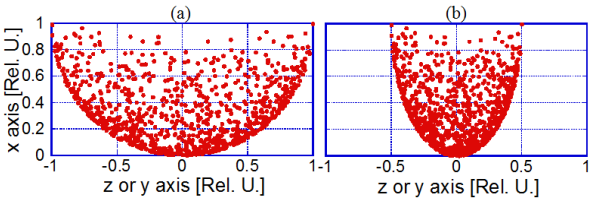

Fig. 8 Schematic of distribution of launched particles: (a) σ_{div} = 1 (cosine distribution), (b) σ_{div} = 1/2.

an index of the axial neutral transport. Because the intensity profile generally does not change as the intensity increase, the best signal-to-noise ratio is obtained at the peak intensity. Thus, this timing is appropriate for obtaining the distribution of emission intensity. We analyzed the FWHM for each SMBI plenum pressure. Figure 5 shows how the FWHM depends on the plenum pressure. All experimental conditions except for the SMBI plenum pressure were fixed. As shown in Fig. 5, the FWHM value decreases with increasing SMBI plenum pressure. These experimental reveal a FWHM of approximately 40 to 56 cm. In the next section, we describe the modeling of SMBI experiments based on experimental results.

4. Simulation Model and Results

We used the Monte-Carlo simulation code DEGAS [5] to analyze the behavior of neutral particle in GAMMA 10 [6]. Three-dimensional mesh-model for DEGAS was applied to the central-cell [7]. Figure 6 shows the result of applying the fully 3-D mesh-model to the central and anchor cells. In this model, the limiters and antennae of the ICRF are precisely implemented in a realistic configuration. Furthermore this mesh model was improved for modeling SMBI experiments; it was expanded around the SMBI port and new mesh was added in a realistic configuration about the SMBI valve. A schematic of the vicinity of the SMBI valve is shown in Fig. 6. The background plasma parameters (T_e, T_i, $n_e = n_i$, etc) on each mesh were determined based on the experimental data, as shown in Fig. 7. The neutral source was introduced at the top of the SMBI valve. The axial distribution of Hα emission was calculated to investigate the neutral transport of SMBI.

To simulate the molecular beam injected by SMBI, we introduce σ_{div} to index the divergence angle of the initial particles. If the angular profile of launched particles has a cosine distribution, the divergence-angle index is $\sigma_{div} = 1$. If $\sigma_{div} = 1/2$, for example, the horizontal component of the velocity vector in the cosine distribution is reduced to half. Figure 8 shows a schematic of the distribution of launched particles for $\sigma_{div} = 1$ (a) and $\sigma_{div} = 1/2$ (b). We find that the experimental result for conventional gas puff is reproduced under the conditions $\sigma_{div} = 1$ [8]. We also investigate the way in which the axial distribution of Hα emission depends on σ_{div}. Figure 9 shows the axial distribution of the Hα emission near the SMBI injection port, as calculated by DEGAS and for three cases of divergence-angle index. As shown in Fig. 9, the simulation results for $\sigma_{div} = 1$ do not agree with the emission FWHM obtained from the experimental results. The simulated and experimental results are compared in Fig. 10. The hatched zone in Fig. 10 shows the FWHM obtained from the experimental results. As shown in Fig. 10, the SMBI must be modeled under the initial particle conditions of $\sigma_{div} = 0.4$ to 0.5 to reproduce the experimental results for a plenum pressure between 0.2 and 1.0 MPa. These results suggest that a difference exists

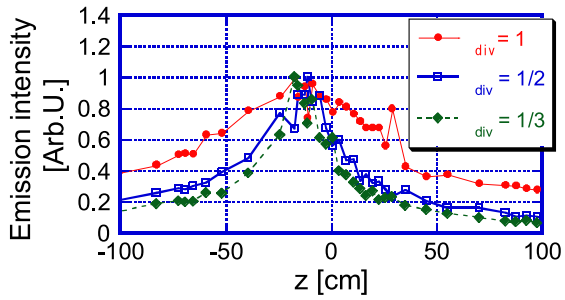

Fig. 9 Axial distribution of Hα emission intensity calculated by DEGAS code for three cases of divergence-angle index.

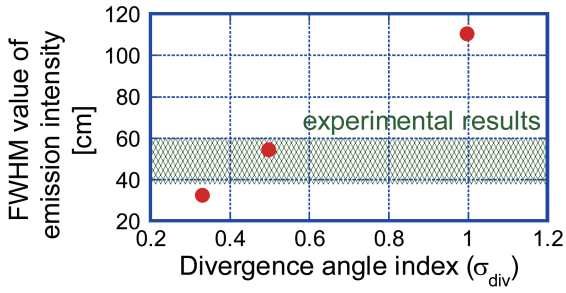

Fig. 10 FWHM of emission as a function of divergence angle. Experimental results are compared with simulation results.

between SMBI and conventional gas puff with regard to the initial conditions of the divergence angle of the initial particles.

5. Summary

Neutral particle transport during SMBI was investigated by using the DEGAS code. The experimental results of SMBI could not be reproduced by simulation for the initial conditions of conventional gas puff. According to experimental results obtained by the high-speed camera, the neutral-particle divergence angle for SMBI must converge more than that for the cosine distribution. The experimental results allowed us to find how to configure particle sources for reproducing SMBI experiments. In addition, we clarified the difference between initial conditions for neutral particles for SMBI and for conventional gas puff.

In future work, a more detail configuration of the particle source will be investigated to discuss the penetration depth of SMBI neutral particle.

Acknowledgments

This study was supported by the bi-directional collaboration research program from the University of Tsukuba, Kyoto University, and Hiroshima University (NIFS11KUGM057, NIFS11KUHL042, NIFS09KUGM033). The authors thank the members of the GAMMA 10 groups for their collaboration in the experiments and their for helpful discussions.

[1] L. Yao, in *New Developments in Nuclear Fusion Research* (Nova Sci. Pub, 2006) p.61.
[2] B. Pégourié *et al.*, J. Nucl. Mater. **313-316**, 539 (2003).
[3] T. Mizuuchi *et al.*, Contrib. Plasma Phys. **50**, No.6-7, 639 (2010).
[4] M. Inutake *et al.*, Phys. Rev. Lett. **55**, 939 (1985).
[5] D. Heifetz, D. Post, M. Petravic *et al.*, J. Comput. Phys. **46**, 309 (1982).
[6] Y. Nakashima *et al.*, J. Nucl. Mater. **196-198**, 493 (1992).
[7] Y. Nakashima *et al.*, J. Plasma Fusion Res. SEREIS **6**, 546 (2004).
[8] Y. Nakashima *et al.*, J. Nucl. Mater. **363-365**, 616 (2007).